Pure & Appl. Chem., Vol. 70, No. 4, pp. 881–888, 1998.
Printed in Great Britain.

Time-resolved resonance Raman study of dioxygen reduction by cytochrome *c* oxidase

Teizo Kitagawa and Takashi Ogura

Institute for Molecular Science, Okazaki National Research Institutes, Myodaiji, Okazaki 444 Japan

Abstract: Six oxygen-associated vibrations were observed for reaction intermediates of bovine cytochrome *c* oxidase with O_2 using time-resolved resonance Raman spectroscopy at room temperature. The isotope frequency shifts for $^{16}O^{18}O$, have established that the primary intermediate is an end-on type dioxygen adduct of Fe_{a3}, which is followed by two oxoheme intermediates, and that the final intermediate appearing around 3 ms is the Fe-OH heme. The reaction rate between the two oxoheme intermediates was significantly slower in D_2O than in H_2O, suggesting tight coupling with proton translocation at this step. It is noted that the reaction intermediates of oxidized enzyme with hydrogen peroxide yields the same three sets of oxygen isotope-sensitive bands as those seen for oxoheme intermediates of the dioxygen reduction, indicating the identity of intermediates.

INTRODUCTION

The terminal oxidase of mitochondrial respiratory chain contains two copper redox centers (Cu_A and Cu_B) and two heme-A groups (Cyt *a* and Cyt a_3) [1] and has been historically called cytochrome aa_3 (E.C. 1.9.3.1). A conceptual structure of this enzyme is illustrated in Fig. 1. The Cu_A center, which is a binuclear complex and shuttles between Cu^ICu^{II} and Cu^ICu^I, receives electrons from cytochorme *c* and gives them to Cyt *a*.. Heme *a* is of a six-coordinate low-spin type and works simply for electron transfer from Cu_A to Cyt a_3, while heme a_3 is of a five-coordinate high-spin type and provides the catalytic site for O_2 reduction. Cu_B is antiferromagnetically coupled with heme a_3 in the resting state and accordingly, is EPR silent, while the role of Cu_B remains to be clarified. Full reduction of O_2 to H_2O needs four electrons and four protons. In a respiration system the reaction is catalyzed by the heme iron of Cyt a_3 (Fe_{a3}) in stepwise, that is, repetitions of one electron transfer to oxygen followed by uptake of one proton [2]. In addition to four consumed protons for yielding two water molecules, another four protons are transported across the mitochondrial inner membrane to generate the electrochemical potential to be used for ATP synthesis from ADP [3,4]. The stepwise reduction of an isolated O_2 molecule may imply generation of intermediately reduced oxygen species like $\cdot O_2^-$, $\cdot OOH$, O_2^{--}, $\cdot OOH^-$, $HOOH$, $\cdot O^-$, and $\cdot OH$, which are called active oxygen and very toxic to organisms, but no such dangerous intermediates are normally released in the respiration process. Then, how is the molecular oxygen reduced in mitochondria and how is the electron trasfer coupled with the proton transport? The purpose of our study is to answer these questions.

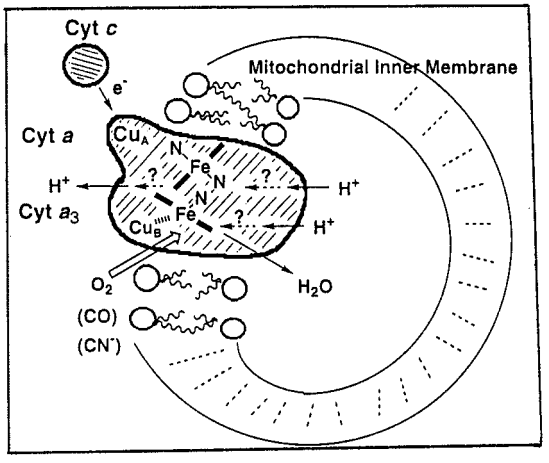

Fig. 1. Concenptual illustration of cytochrome *c* oxidase. The enzyme is located in the inner membrane of mitochondria and is functionally categorized into two parts, that is, cytochrome *a* (Cyt a) and cytochrome a_3 (Cyt a_3). Cytocrome *c* gives electrons to Cu_A, which actually consists of binuclear copper center. Electrons are transferred from Cu_A to the six-coordinate heme (Cyt a) and then to the five-coordinate heme (Cyt a_3). Cu_B is anti-ferromagnetically coupled with the iron of Cyt a_3 in the resting state. O_2 binds to the Fe^{II} ion of Cyt a_3 to which CO and CN^- also can be bound. Upon reduction of one O_2 molecule, four protons are translocated across the membrane from the matrix- to cytosol side and in addition, four protons are consumed in the matrix side to generate two water molecules.

The three dimensional structure of bovine cytochorme *c* oxidase (CcO) with $M_r = 2 \times 10^5$ and 13 subunits has been revealed recently with X-ray crystallography [5]. The reaction mechanism of this enzyme has been investigated with various spectroscopic techniques including time-resolved [6-8] and cryo-trapped absorption [9], and EPR [10,11] spectroscopy but more recently a breakthrough was made with time-resolved resonance Raman (TR^3) spectroscopy by Babcock' group [12,13], Rousseau' group [14,15] and our group [16-19]. The course of progress has been summarized in a comprehensive review article [20] and here, some hot results from our TR^3 experiments [19] are explained.

REACTION OF REDUCED CcO WITH O_2

Time-Resolved Resonance Raman Spectra

Resonance Raman (RR) spectroscopy allows to observe selectively the vibrational spectra of a chromophore by tuning the excitation wavelength into an absorption band of a molecule. Application of this technique to heme proteins has brought about unique and important information on dynamical as well as static structures [21]. In the time resolved measurements, the reaction was initiated by photolysis of CO-inhibited CcO in the presence of O_2 and after a certain delay time (Δt_d) RR spectra were determined. In this TR^3 experiments, a device for simultaneous measurements of Raman and absorption spectra [22] and a sample circulation system for regenerating the reacted enzyme during one cycle [18] were constructed. Since the Raman intensities of the oxygen-associated vibrations are extremely weak, we measured the RR spectra of intermediates for $^{16}O_2$ and $^{18}O_2$ at the same time under an identical condition and calculated their differences.

Figure 2 shows the TR^3 spectra observed with the delay times of 0.1 (A), 0.27 (B), 0.54 (C), 2.7 (D) and 5.4 ms (E) for the H_2O solution at 3 °C [19]. The visible absorption spectrum simultaneously observed with spectrum (A) is close to that of Compound A obtained in cryogenic techniques[9]. Spectrum (A) shows the Fe-O_2 stretching ($\nu_{Fe\text{-}O2}$) RR bands at 571/544 cm^{-1} for the $^{16}O_2/^{18}O_2$ derivatives. The frequencies and isotope shift are very close to those seen for HbO_2 and MbO_2 [23]. In the next stage (Δt_d=0.27 ms), new Raman bands appear at 804/764, 785/750, and 356/342 cm^{-1}. Spectrum (D) which exibits only the 785/750 cm^{-1} pair

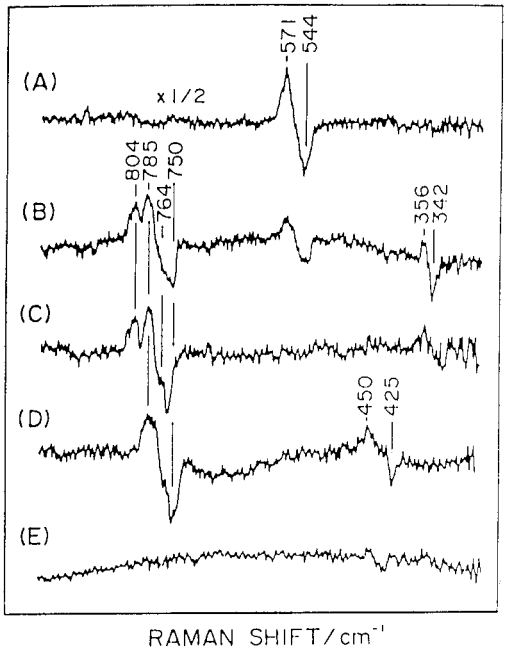

Fig. 2. TR^3 difference spectra of reaction intermediates of CcO in H_2O. The Raman difference spectra obtained by subtracting the spectrum of the corresponding $^{18}O_2$ derivative from the spectrum of $^{16}O_2$ derivative at each delay time are depicted. Therefore, positive and negative peaks denote the contributions of $^{16}O_2$- and $^{18}O_2$-derivatives, respectively. Delay time after initiation of the reaction is 0.1 (A), 0.27 (B), 0.54 (C), 2.7 (D) and 5.4 ms (E). Excitation wavelength, 423 nm; Temperature, 3 °C. (Taken from Ref. 19).

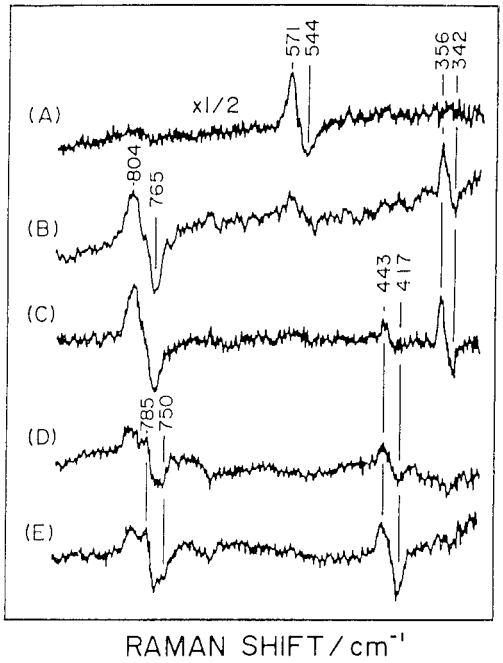

Fig. 3. TR^3 difference spectra of reaction intermediates of CcO in D_2O. Delay time is 0.1 (A), 0.54 (B), 2.7 (C), 6.5 (D) and 11 ms (E). Other conditions are the same as those for Fig. 2. (Taken from Ref. 19).

near 800 cm^{-1} strongly suggests that the 804/764 cm^{-1} pair precedes the 785/750 cm^{-1} pair. The 450/425 cm^{-1} pair, which arises from the Fe-OH stretch ($\nu_{Fe\text{-}OH}$) of the Fe_{a3}^{III}-OH heme [13,15,17], appears at Δt_d=2.7 ms, but disappears at Δt_d=5.4 ms due to exchanges of the bound $^{18}OH^-$ anion with bulk water. This $\nu_{Fe\text{-}OH}$ frequency is significantly lower than those of aquametHb and aquametMb at 495 ad 490 cm^{-1}, respectively [24], presumably due to strong interaction between the bound OH^- group and Cu_B.

Figure 3 shows similar difference RR spectra observed with Δt_d=0.1 (A), 0.54 (B), 2.7 (C), 6.5 (D) and 11 ms (E) for the D_2O solution at 3 °C. The $\nu_{Fe\text{-}O2}$ frequencies in spectrum (A) are the same as those in Fig. 2(A). With the delay times of Δt_d=0.54 (B) and 2.7 ms (C), however, a single differential band was observed around 800 cm^{-1} (at 804/764 cm^{-1}), contrary to the case for the H_2O solution. Therefore, it was misunderstood once [18] that the 785/750 cm^{-1} bands in the H_2O solution were shifted to 796/766 cm^{-1} in D_2O, giving rise to an overlapping band centered around 800 cm^{-1}. However, it turned out from Fig. 3 that the lifetime of the 804/764 cm^{-1} species is so different between the H_2O and D_2O solutions that the 785/750 cm^{-1} species was not generated in D_2O yet at Δt_d=2.7 ms. It is noted that the 356/342 cm^{-1} bands are clearly seen in spectra (B) and (C) at the same frequencies as those in the H_2O solution. Spectra (D) and (E) for the D_2O solution demonstrated that the 785/750 cm^{-1} bands did appear at the same frequencies but much later than those in the H_2O solution. It is estimated that the conversion rate from the 804/764 cm^{-1} species to the 785/750 cm^{-1} species in D_2O is approximately one fifth of that in H_2O. The subsequent appearance of the 443/417 cm^{-1} bands, which arise from the Fe-OD stretch, is consistent with the results shown in Fig. 2. The experiments with Δt_d=0.3~0.5 ms for D_2O solutions (data not shown) yielded the 804/764 and 356/342 cm^{-1} bands in a manner similar to spectrum (B).

When the mixed valence CO-bound enzyme, which had only two electrons in a molecule, was used as a starting compound instead of the fully reduced CO-bound enzyme, which had four electrons, the primary intermediate gave the O_2-isotope-sensitive bands at 571/544 cm^{-1} [25,26]. The subsequent intermediate, which is characterized by the difference absorption peak at 607 nm (intermediates - fully oxidized), was found to give RR bands at 804/764 and 356/342 cm^{-1} for $^{16}O_2/^{18}O_2$ [19]. These bands lasted as long as Δt_d=4.2 ms but the bands at 785/750 and 450/425 cm^{-1} did not appear in this case. These results have proved that the species giving rise to the 804/764 cm^{-1} pair has an oxidation state higher than that of the 785/750 cm^{-1} species. Hirota et al. [27] carried out similar TR^3 experiments for the reaction intermediates of fully reduced *E. coli* cytochrome *bo* with O_2, and found the O_2-isotope-sensitive bands at 568/535, 788/751, and 361/347 cm^{-1} but not those corresponding to the bands of cytochrome aa_3 at 804/764 cm^{-1}, presumably owing to very short lifetime.

Binding Geometry of O_2

In order to determine whether the dioxygen adduct of CcO adopts the side-on or end-on geometry, Ogura et al. [18] examined RR spectra of $^{16}O^{18}O$-bound CcO. The results

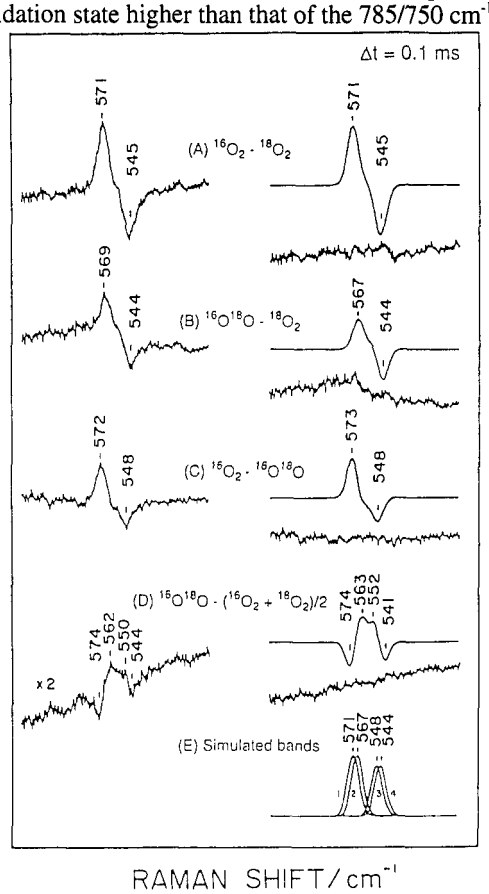

Fig. 4. TR^3 difference spectra in the Fe^{III}-O_2^- stretching region of CcO at the delay time of 0.1 ms. left side: observed spectra; right side: calculated spectra; (A) $^{16}O_2$ - $^{18}O_2$; (B) $^{16}O^{18}O$ - $^{18}O_2$; (C) $^{16}O_2$ - $^{16}O^{18}O$; (D) $^{16}O^{18}O$ - ($^{16}O_2$ + $^{18}O_2$)/2. (E) The Fe-$^{16}O_2$ (1), Fe-$^{16}O^{18}O$ (2), Fe-$^{18}O^{16}O$ (3), and Fe-$^{18}O_2$ (4) stretching Raman bands assumed for the simulation. Their peak intensity ratios are 6:6:5:5, and all have a Gaussian band shape with a FWHM of 12.9 cm^{-1}. In the calculation for the $^{16}O^{18}O$ spectrum, (spectrum 2 + spectrum 3)/2 was used. The differences between the observed and calculated spectra are depicted with the same ordinate scale as that of the observed spectra under the individual calculated spectra. experimental conditions: probe beam, 423 nm, 4 mW; pump beam, 590 nm, 210 mW; accumulation time, 4800 s. (Taken from Ref. 18).

are shown in Fig. 4, where the observed and simulated isotope-difference spectra are depicted on the left and right sides, respectively, and the combination of the isotope species in the difference calculations is specified in the middle. If $^{16}O^{18}O$ binds to Fe_{a3}^{II} in an end-on geometry, the $\nu_{Fe\text{-}O2}$ frequencies for Fe-^{16}O-^{18}O and Fe-^{18}O-^{16}O should be different. Since these two species will be generated by equal amounts, two $\nu_{Fe\text{-}O2}$ RR bands should appear. On the other hand, if the binding is of an side-on type, the $\nu_{Fe\text{-}O2}$ frequencies for Fe($^{16}O^{18}O$) and Fe($^{18}O^{16}O$) are identical and are located in the middle of the $\nu_{Fe\text{-}O2}$ frequencies of the $^{16}O_2$- and $^{18}O_2$-adducts.

The difference-peak intensities in spectra (B) and (C) are weaker than those in spectrum (A) and peak frequencies are slightly different. If it is assumed that the $^{16}O_2$ and $^{18}O_2$ species give a single $\nu_{Fe\text{-}O2}$ RR band at 571 and 544 cm^{-1}, respectively, but the$^{16}O^{18}O$ species gives two $\nu_{Fe\text{-}O2}$ bands at 567 and 548 cm^{-1} with Gaussian band shapes ($\Delta\nu_{1/2}$=12.9 cm^{-1}) and intensities as representedby spectra (E), the difference calculations for the combinations specified for (A) through (D) yielded the patterns as delineated on the right side. The residuals in the subtraction of the simulated spectrum from the observed spectrum are depicted below each simulated spectrum. The calculated difference spectrum, $^{16}O^{18}O$ - ($^{16}O_2$+$^{18}O_2$)/2 (spectrum D), gives positive peaks at 563 and 552 cm^{-1} and troughs at 574 and 541 cm^{-1}, which are in good agreement with the observed spectra. This suggests that the Fe-O_2 stretching frequencies for the Fe-^{16}O-^{18}O and Fe-^{18}O-^{16}O species are 567 and 548 cm^{-1}, respectively. The magnitude of the isotopic frequency shifts and the simple normal coordinate calculations allowed us to estimate the Fe-O-O bond angle to be nearly 120° similar to that in HbO_2 and MbO_2. Thus, this experiment established that the binding of O_2 to Fe_{a3} in CcO·O_2 is of the end-on type.

Assignments of Transient RR Bands Around 800 cm^{-1}

Spectra (B) and (C) in Fig. 2 at Δt_d=0.27 and 0.54 ms give two oxygen-isotope sensitive bands around 800 cm^{-1}, and the higher frequency component arises from the species with the Fe^{V} oxidation level (compound I of peroxidase). In this frequency region , two kinds of oxygen-associated bands are expected; one is the peroxy O^{-}-O^{-} stretch (ν_{OO}) and the other is an ironoxo Fe=O stretch ($\nu_{Fe=O}$). These two modes cannot be distinguished by the $^{16}O_2$ and $^{18}O_2$ isotopic frequency shifts. However, if $^{16}O^{18}O$ is used to produce such intermediates, the distinction would be possible. The peroxy intermediate for $^{16}O^{18}O$ is expected to give an additional ν_{OO} band in a middle of those for the $^{16}O_2$ and $^{18}O_2$ derivatives. In contrast, the oxo intermediate for $^{16}O^{18}O$ is expected to yield two bands at the same frequencies as those seen for the $^{16}O_2$ and $^{18}O_2$ derivatives but with half intensity.

Such a distinction was satisfactorily carried out with $^{16}O^{18}O$ on the 804/764 and 785/750 cm^{-1} bands. The results are shown in Fig. 5, where the TR^3 difference spectra observed with Δt_d=1.1 ms at 5 °C for the H_2O and D_2O solutions are presented on the left and right sides, respectively. The various isotope combinations

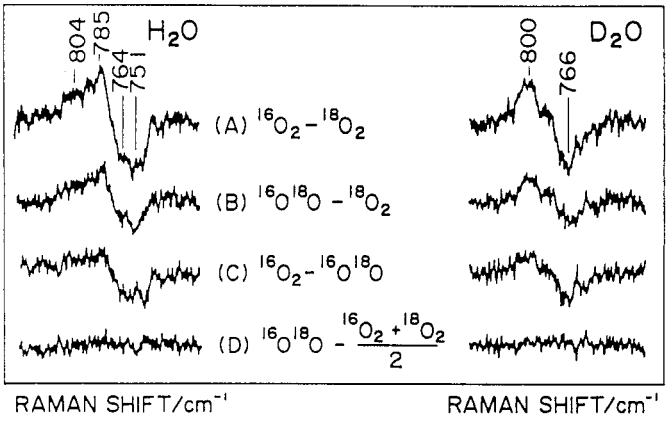

Fig. 5. Higher resolution TR^3 difference spectra of CcO reaction intermediates in the ~800 cm^{-1} region for the delay time of 1.1 ms at 5 °C for H_2O (left) and D_2O solutions (right). The ordinate scales are common to all spectra. The spectra combined in the difference calculations are specified in the middle of the figure. Resolution, 0.43 cm^{-1}/channel. (Taken from Ref. 18).

are defined in the center of the figure. In trace (A) for the H_2O solution, there are two bands at 804 and 785 cm^{-1} for $^{16}O_2$ and they are downshifted to 764 and 751 cm^{-1} with $^{18}O_2$, in agreement with Fig. 2(B), obtained in independent experiments with different batches of the enzyme preparations. It is evident that the peak positions and spectral patterns of the difference spectra (B) and (C) in Fig. 5 for the H_2O solution are alike and similar to those of spectrum (A) but their intensities are approximately half of those in spectrum (A). The same features are also seen for the D_2O solution (right side). The point to be emphasized is that there is no difference peak in the bottom traces for either the H_2O or D_2O solution. This feature definitely differs from that seen in Fig. 4(D).

These results indicate that only one atom of O_2 is primarily responsible for the two RR bands. In other words, neither of the bands at 804/764 nor 785/750 cm^{-1} are assignable to the O-O stretching mode. Although the two sets of RR bands arise from an Fe=O stretch, electronic properties of their hemes seem to be distinct, because the 804/764 cm^{-1} bands, but not the 785/750 cm^{-1} bands, were clearly identified upon Raman excitation at 607 and 441.6 nm, but only the 785/750 cm^{-1} bands were observed upon excitation at 567.1 nm.

Assignment of the Transient Band Around 350 cm^{-1}

Relative intensities of the 804/764 and 356/342 cm^{-1} bands are altered with the delay time and, upon excitation at 441.6 nm, the 356/342 cm^{-1} bands are not enhanced while the 804/764 cm^{-1} bands are clearly observed. Therefore, the two sets of bands are considered to arise from separate molecular species. To clarify the assignment of this band, Ogura et al. [18] examined the $^{16}O^{18}O$ effect on the 356/342 cm^{-1} bands. The results are shown in Fig. 6, where spectra (A-D) were obtained for the indicated (in the figure) combinations of O_2-isotopes in the H_2O solution and spectrum (E) was obtained for combination (A) in the D_2O solution. Spectra in Figs. 5 are 6 are represented on the same wavenumber scale. It is noticed that the 356 cm^{-1} band is very narrow. The inset of Fig. 6 (spectra A' and E') shows redrawing of spectra (A) and (E) with the wavenumber axis expanded by 2.5 fold. The 356 cm^{-1} band appears to be somewhat broader in D_2O than in H_2O, but both spectra exhibit a flat region between the positive and negative peaks. This means that the separation between the $^{16}O_2$ and $^{18}O_2$ peaks is larger than their bandwidths, and thus the narrowness of the band is not the consequence of the close proximity of the $^{16}O_2$ and $^{18}O_2$ bands. This also means that the peak positions of the difference spectrum correctly represent those of each spectrum.

It is evident from spectrum (E) that there are no deuteration effects on the absolute frequencies of the 356/342 cm^{-1} bands. Therefore, this band cannot be a Cu-OH stretching mode. As was seen for the bands around 800 cm^{-1}, spectra (B) and (C) do not differ from each other in shape or position of the peaks, which are also close to those of spectrum (A). If the 356/342 cm^{-1} bands arose from the Fe-OOH stretch, the frequency difference between the Fe-$^{16}O^{18}OH$ and Fe-$^{16}O^{16}OH$ streches and that between the Fe-$^{18}O^{16}OH$ and Fe-$^{18}O^{18}OH$ stretches should be as large as 2.5 cm^{-1} unless the Fe-O-O bond-angle is close to 90°, and there should be some difference peaks in Fig. 6(D) as seen for the Fe-O_2 adduct in Fig. 4(D). Actually, however, there is no difference peak in spectrum (D) in Fig. 6. Therefore, only one oxygen atom from the O_2 molecule is primarily responsible for the 356 cm^{-1} band, too.

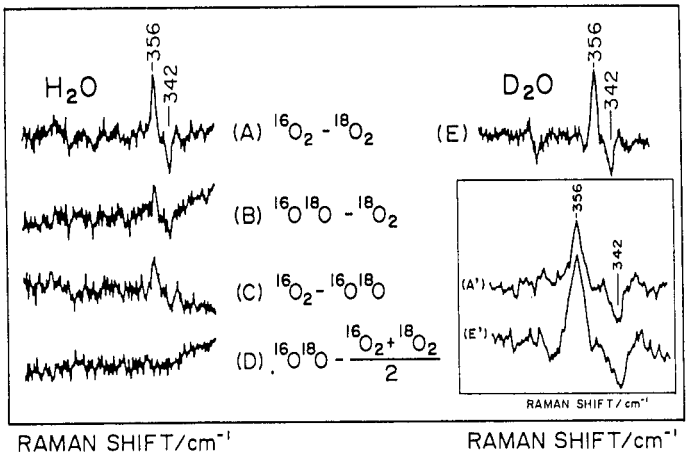

Fig. 6. TR[3] difference spectra of CcO reaction intermediates in the ~350 cm^{-1} region for Δt_d = 0.5 ms at 5 °C for H_2O (left) and D_2O solutions (right). The ordinate scales are common to all spectra. The spectra combined in the difference calculations are specified in the middle of the figure. The inset depicts the plots of spectra A and E expanded by a factor of 2.5 in the wavenumber axis. (Taken from Ref. 18).

REACTION OF OXIDIZED CcO WITH H_2O_2

The reaction of ferric heme proteins with H_2O_2 usually yields the Fe^V-level intermediate first, which is then successively reduced to the Fe^{IV} and Fe^{III} oxidation levels. The reaction of oxidized CcO with H_2O_2 has been extensively studied with visible absorption [28], EPR [29] and RR [30-32]. The visible absorption spectra of reaction intermediates are displayed in Fig. 7, where the differences between the intermediates and fully oxidized enzyme for several delay times are depicted [31]. The so-called "607 nm" form is generated first and then it is replaced by the "580 nm" form. This feature is more clearly seen in the inset, where the difference absorbances at 607 and 578 nm with regard to those of the fully oxidized form are plotted against time. The rate of formation of the "607 nm" form was found to be proportional to the concentration of H_2O_2 and was considered to be the primary intermediate in this reation. This fact means that the "607 nm" form has the Fe^V oxidation level of the heme a_3. When the concentration of H_2O_2 is increased, the "580 nm" form is developed rapidly. This is interpreted in the following way. Under high concentrations of H_2O_2, the "607 nm" form developes much faster and the extra H_2O_2 acts as a reductant to the "607 nm" form to yield the "580 nm" form, which has the Fe^{IV} oxidation level of the heme a_3. Accordingly, relative populations of the "607 nm" and "580 nm" forms can be regulated by the concentration of H_2O_2 and pH [32].

Figure 8 shows the absorption (right) and Soret-excited RR spectra (left) of intermediates which were measured simultaneously with an improved Raman/absorption simultaneous measurement device [30]. In this experiment the concentrations of reaction intermediates in question are retained in a steady state for a certain period of time by adding H_2O_2 at a constant rate to the circulating solution. The upper spectra were obtained under the conditions where the "607 nm" form is dominant, while the lower spectra were obtained under the conditions where the "580 nm" form is dominant. Both RR spectra are represented as the difference between the derivatives obtained from $H_2{}^{16}O_2$ and $H_2{}^{18}O_2$, and accordingly positive and negative peaks correspond to the vibrations associated with ^{16}O and ^{18}O, respectively. It is noted that when the "607 nm" form is dominant, the 804/769 cm^{-1} bands are clearly observed and when the "580 nm" form is dominant, broad bands centered around 785/750 cm^{-1} and sharp bands at 355/340 cm^{-1} are intensified. The intensity of the 355/340 cm^{-1} bands relative to those of the 804/769 and 785/750 cm^{-1} bands were varied with each experiment. This strongly suggested that the species giving rise to the 355/340 cm^{-1} bands also gives a difference band around 800/760 cm^{-1} but is different from the two species giving rise to the 804/769 and 785/750 cm^{-1} bands. The 355/340 cm^{-1} species seems to have an absorption spectrum similar to that of the "580 nm" form. This implies that the "580 nm" form consists of multiple intermediate species [32]. It is stressed that all these oxygen isotope-sensitive bands are identical with those observed in the dioxygen reduction.

Hitherto the "607 nm" form has been believed to be a peroxo species, namely, Fe-O-O-X (X = H or Cu_B). Since both the O^--O^- and Fe=O stretching frequencies are located around 800 cm^{-1}, it is impossible to determine which type of vibrations was observed for the "607 nm" form in Fig. 8. In order to sort out between the two possible modes, experiments using $H_2{}^{16}O^{18}O$ have been performed. The results are shown in Fig. 9, where RR spectra of the "607 nm" form excited at 607 nm are displayed for intermediates derived with $H_2{}^{16}O_2$ (A), $H_2{}^{18}O_2$ (B), and $H_2{}^{16}O^{18}O$ (C) [31]. The band of the $H_2{}^{16}O_2$ derivative at 803 cm^{-1} (A) is shifted to 769 cm^{-1} for the $H_2{}^{18}O_2$ derivative (B), while other bands arising from the porphyrin macrocycle remain unshifted. This is most clearly seen in the difference spectrum (D) (= spectrum (A) - spectrum (B)). The inset shows the same difference spectrum in a wider spectral range (930 - 550 cm^{-1}). It is evident that there is no other oxygen associated band in this frequency region.

In spectrum (C) for the $H_2{}^{16}O^{18}O$ derivative, there are two bands at 803 and 769 cm^{-1}, and their intensities relative to the

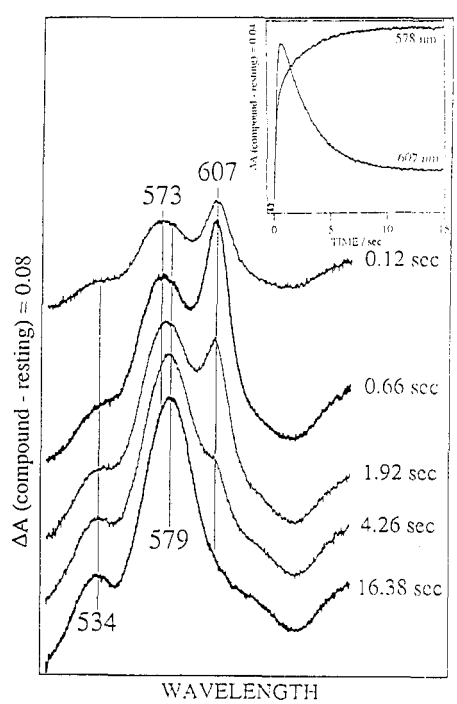

Fig. 7. Transient absorption spectra for reaction intermediates of oxidized CcO with H_2O_2. The spectra are represented as difference spectra with regard to the spectrum of fully oxidized enzyme and delay times after initiation of the reaction are specified at the right side of each spectrum. The zero line for each spectrum is shifted for clear presentation. Inset depicts the behavior of absorbances at 607 and 578 nm against delay times. (Full scale of ΔA is 0.04 in terms of the difference, intermediate minus fully oxidized). (Taken from Ref. 31).

porphyrin bands are reduced to half of those in spectra (A) and (B). This is most clearly seen by the difference spectrum (E) [= spectrum (C) - (spectrum (A) + spectrum (B))/2], which exhibits no band in the 700 - 900 cm^{-1} region. This means that the 803/769 cm^{-1} bands arise from a species which has a single oxygen atom on the heme iron. Consequently, the peroxide structure (Fe-O-O-X), postulated for the "607 nm" form, was proved to be no longer valid.

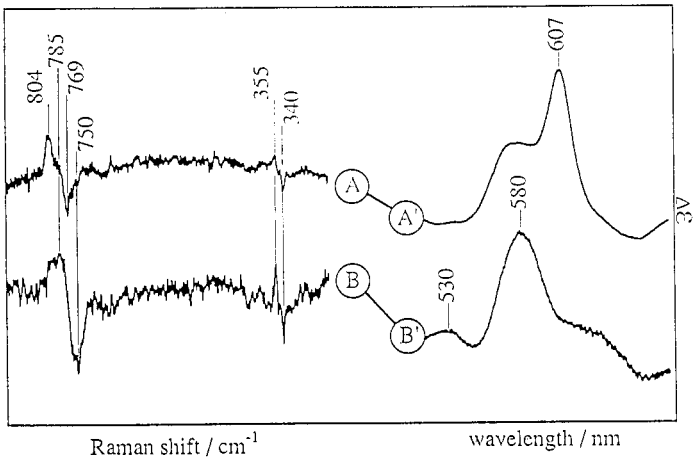

Fig. 8. The steady-state Raman/absorption simultaneously observed spectra of the "607 nm" and "580 nm" forms of cytochrome *c* oxidase at pH 8.5. Raman spectra A and B are shown as a difference of $H_2{}^{16}O_2$ compound minus $H_2{}^{18}O_2$ compound. Spectra A/A': laser, 427 nm, 2.5 mW; accumulation time, 3x2400 sec for each isotope; cytochrome *c* oxidase, 50 μM; initial concentration of H_2O_2, 1 mM, Spectra B/B': laser power, 7.5 mW; accumulation time, 3x800 sec for each isotope; cytcohrome *c* oxidase, 10 μM; initial concentration of H_2O_2, 5 mM. Absorption spectra are represented as a difference with regard to the spectrum of the resting enzyme; ordinate full scale $\Delta\varepsilon$ = 11.7 mM^{-1} cm^{-1}; pathlength 0.6 mm. (Taken from Ref. 30).

CONCLUSION

The reaction intermediates of CcO characterized by RR spectroscopy and other spectroscopic techniques are inter-related in Fig. 10, where the oxygen-associated frequencies for $^{16}O/^{18}O$ are also specified. Two kinds of reactions, that is, dioxygen cycle (right) and peroxide cycle (left) were treated in this article. The first intermediate in the reaction of reduced CcO with O_2, which has been called Compound A has now been demonstrated to be a dioxygen adduct of cytochrome a_3 with $\nu_{Fe\text{-}O2}$ at 571 cm^{-1}. The binding of O_2 is of an end-on type. The subsequent intermediates, called Compound B might be mixtures of intermediates and it is difficult to correlate them with a species with specific oxygen-isotope-sensitive bands which are observed at 804, 356, and 785 cm^{-1} for $^{16}O_2$ in the order of their appearance. The intermediate which is generated in the reaction of mixed-valence enzyme with O_2, gives the oxygen-isotope-sensitive bands at 804 and 356 cm^{-1}. The final intermediate in the dioxygen cycle has an $Fe_{a3}{}^{III}$-OH^- heme with $\nu_{Fe\text{-}OH}$ RR band at 450 cm^{-1}. This OH^- group is exchangeable with bulk water.

In the reaction of oxidized enzyme with H_2O_2, the first intermediate, the "607 nm" form, has long been thought to have the peroxo Fe_{a3}-O-O-X structure, but RR experiments demonstrated that it contains an oxoiron heme. The subsequent intermediates give a broad difference peak at 580 nm and seem to have multiple components. RR spectroscopy can sort out two species within the "580 nm" form. One gives the oxygen-isotope-

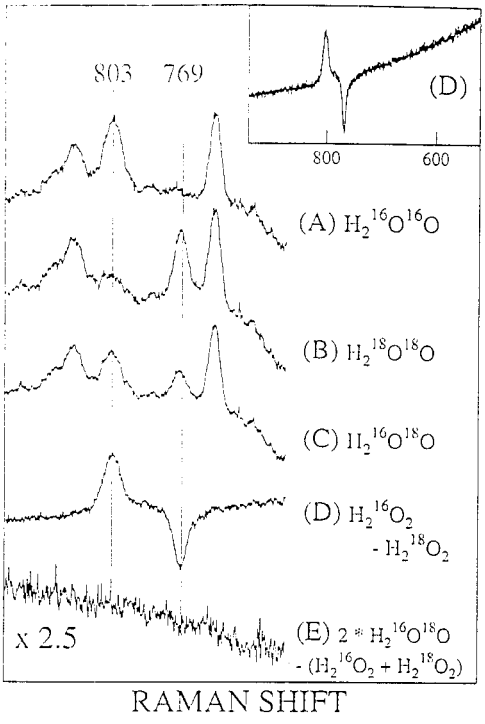

Fig. 9. The 607-nm excited steady-state RR spectra in the 800 cm^{-1} region of the "607 nm" form of CcO formed in the reaction of the oxidized enzyme with hydrogen peroxide. Hydrogen peroxide used are $H_2{}^{16}O_2$ (A), $H_2{}^{18}O_2$ (B), and $H_2{}^{16}O{}^{18}O$ (C). Spectra D and E show difference spectra: spectrum D = spectrum A - spectrum B; spectrum E = spectrum C - (spectrum A + spectrum B)/2. The inset (Spectrum D) is the same as spectrum D in the main frame but shows the full frequency range measured. Experimental conditions; cross section of flow cell, 0.6x0.6 mm^2; slit width, 4.2 cm^{-1}; laser 607 nm, 100 mW at the sample; total accumulation time, 78, 78, and 156 min for spectra A, B and C, respectively, and 160 min for the resting enzyme; cytochrome *c* oxidase, 50 μM, pH 7.45. (Taken from Ref. 31).

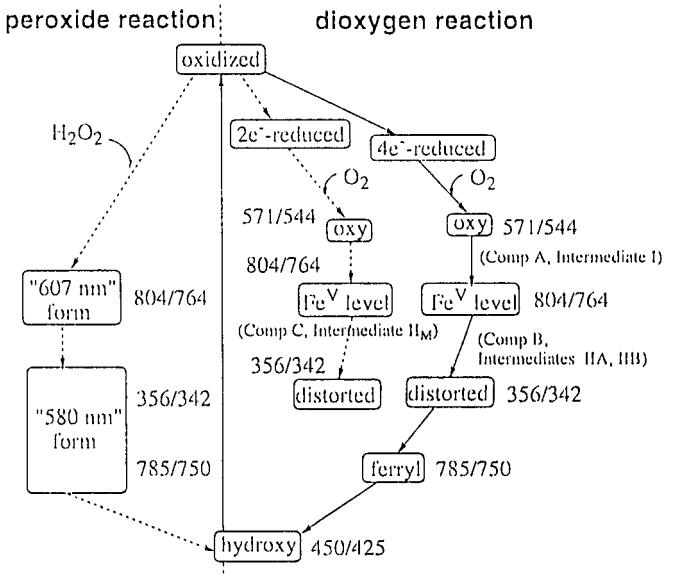

Fig. 10. Reaction mechanism of cytochrome *c* oxidase, inter-relations of intermediates obtained with different techniques, and the specific oxygen-associated vibrational frequencies ($^{16}O_2$ derivatives/$^{18}O_2$ derivatives in cm^{-1} unit) of individual intermediates. In the dioxygen reaction the fully reduced (4e⁻-reduced) and the mixed-valence (2e⁻-reduced) species are contained. The peroxide reacion gives rise to two absorption forms, but the "580 nm" form is of multiple species and is further sorted out by vibrational frequencies. The "peroxy" and "ferryl" forms in the reversed reaction are presumably the same as the "607 nm" and 580 nm" forms of the peroxide reaction, respectively.

sensitive bands at 356 and ~800 cm^{-1} and the other gives the band at 785 cm^{-1}. The latter is unquestionably assigned to the Fe^{IV}=O stretching mode.

REFERENCES

1. M.Wikstrom, K.Krab, and M.Saraste.*Cytochrome Oxidase; A Synthesis* , Academic Press, New York (1981).
2. G. T. Babcock and M. Wikstrom. *Nature*, **356**, 301-309 (1992).
3. M.Wikstrom. *Proc.Natl. Acad. Sci. U.S.A.* **78**, 4051-4055 (1981).
4. N.Sone and P.C.Hinkle. *J. Biol. Chem.* **257**, 12600-12604 (1982).
5. T.Tsukihara, H.Aoyama, E.Yamashita, T.Tomizaki, H.Yamaguchi, K.Shinzawa-Itoh,R.Nakashima, R.Yaono, and S.Yoshikawa. *Science* **269**, 1069-1074 (1995).
6. Y. Orii *Ann. N. Y. Acad. Sci.*, **550**, 105-117 (1988).
7. R. S. Blackmore, C. Greenwood and Q. H. Gibson J. Biol. Chem. **266**, 19245-19249 (1991).
8. M. Oliveberg and B. G. Malmstrom. *Biochemistry*, **31**, 3560 (1992).
9. B. Chance, C. Saronio and J. S. Leigh, Jr. *J. Biol. Chem.*, **250**, 9226-9237 (1975).
10. G. M. Clore, L. -E. Andreasson, B. Karlsson, R. Aasa, and B. G. Malmstrom.*Biochem. J.*, **185**, 139-154 (1980).
11. D. F. Blair, S. N. Witt and S. I. Chan. *J. Am. Chem. Soc.*, **107**, 7389-7399 (1985).
12. C. Varotsis, W. H. Woodruff and G. T. Babcock. *J. Am. Chem. Soc.*, **111**, 6439; (1989) **112**:1297 (1990).
13. C. Varotsis, Y. Zhang, E. H. Appelman and G. T. Babcock. *Proc. Natl. Acad. Sci. U.S.A.*, **90**, 237 (1993).
14. S. Han, Y. -c. Ching and D. L. Rousseau. *Proc. Natl. Acad.Sci. U.S.A.*, **87**, 2491-2495 (1990).
15. S. Han, Y. -c. Ching and D. L. Rousseau. *Nature*, **348**, 89-90 (1990).
16. T. Ogura, S. Takahashi, K. Shinzawa-Itoh, S. Yoshikawa and T. Kitagawa. *J. Am. Chem. Soc.*, 112:5630-5631 (1990).
17. T. Ogura, S. Takahashi, K. Shinzawa-Itoh, S. Yoshikawa and T. Kitagawa. *Bull. Chem. Soc. Jpn.*, **64**, 2901-2907 (1991).
18. T. Ogura, S. Takahashi, S. Hirota, K. Shinzawa-Itoh, S. Yoshikawa, E. H. Appelmanand T. Kitagawa. *J. Am. Chem. Soc.*, **115**, 8527-8536 (1993).
19. T. Ogura, S. Hirota, D. A. Proshlyakov, K. Shinzawa-Itoh, S. Yoshikawa and T. Kitagawa. *J. Am. Chem Soc.* **118**, 5443-5449 (1996).
20. T. Kitagawa, and T. Ogura. *Progr. Inorg. Chem.* **45**, 431-479 (1997).
21. T. Kitagawa and T. Ogura *Adv. Spectrosc.* **21**, 139-188 (1993).
22. T. Ogura, and T. Kitagawa. *Rev. Sci. Instrum.* **59**, 1316-1320 (1988)..
23. K. Nagai, T. Kitagawa and H. Morimoto. *J. Mol. Biol.*, **136**, 271-289 (1980)..
24. S. A. Asher and T. M. Schuster. *Biochemistry*, **18**, 5377-5387 (1979).
25. S. Han, Y. -c. Ching and D. L. Rousseau. *J. Am. Chem. Soc.*, **112**, 9445-9450 (1990).
26. C. Varotosis, W. H. Woodruff and G. T. Babcock. *J. Biol. Chem.*, **265**, 11131-11136 (1990).
27. S.Hirota, T. Mogi, T. Ogura, T. Hirano, Y.Anraku, and T. Kitagawa. *FEBS Lett.* **352**, 67-70 (1994).
28. T. V. Vygodina and A. A. Konstantinov. *Ann. N. Y. Acad. Sci.*, **550**, 124-138 (1988).
29. M. Fabian and G. Palmer. *Biochemistry* **34**, 13802-13810 (1995).
30. D. A. Proshlyakov, T. Ogura, K. Shinzawa-Itoh, S. Yoshikawa, and T. Kitagawa. *Biochemistry* **35**, 76-82 (1996).
31. D. A. Proshlyakov, T. Ogura, K. Shinzawa-Itoh, S. Yoshikawa, E. H. Appelman and T. Kitagawa. *J. Biol. Chem.*, **269**, 29385-29388 (1994).
32. D. A. Proshlyakov, T. Ogura, K. Shinzawa-Itoh, S. Yoshikawa and T. Kitagawa. *Biochemistry* **35**, 8580-8586 (1996).